Journal of Integrative Neuroscience

J. Integr. Neurosci. **2023**; 22(6): 136
https://doi.org/10.31083/j.jin2206136

Original Research

Identification of a lncRNA/circRNA-miRNA-mRNA ceRNA Network in Alzheimer's Disease

Lining Su[1], Yixuan Zhang[1], Yanbing Wang[2,*], Huiping Wei[1,*]

[1]Department of Basic Medicine, Hebei North University, 075000 Zhangjiakou, Hebei, China
[2]Department of Sports, Hebei North University, 075000 Zhangjiakou, Hebei, China
*Correspondence: wangyanbingtyb2010@163.com (Yanbing Wang); 1931451387@qq.com (Huiping Wei)
Academic Editor: Gernot Riedel
Submitted: 28 March 2023 Revised: 11 May 2023 Accepted: 16 May 2023 Published: 17 October 2023

Abstract

Background: Alzheimer's disease (AD) occurs in the elderly and pre-elderly, characterized by decline of memory, cognitive dysfunction, impairment of learning capacity, and motor dysfunction. Recently a competitive endogenous RNA (ceRNA) network has been found to be related to AD progression, but there is still little understanding of the ceRNA regulatory network in AD. This study aims to explore the important regulatory mechanisms of ceRNA regulatory networks containing long non-coding RNAs (lncRNAs), circular RNAs (circRNAs), microRNAs (miRNAs), and messenger RNAs (mRNAs) in AD. **Methods**: Data from the gene expression omnibus (GEO) database were used for the analysis. To study enrichment function for the upregulated and downregulated mRNAs, Gene Ontology (GO) and Kyoto Encyclopedia of Genes and Genomes (KEGG) enrichment analyses were performed using the Metascape database, respectively. Based on the STRING database and Cytoscape software 3.9.1, a protein-protein interaction (PPI) network was constructed. The hub genes in this network were identified utilizing the CytoHubba plugin in Cytoscape. The TargetScan, miRWalk, and miRDB were selected to calculate the regulatory interaction between miRNAs and the hub genes. LncRNAs were predicted using RNA22. Additionally, circRNA prediction was executed using the circBank database. **Results**: 711 downregulated and 670 upregulated overlapping mRNAs were identified between AD and control samples. 32 downregulated and 340 upregulated miRNAs were obtained from AD samples compared with control samples. 78 upregulated and 205 downregulated circRNAs were screened. 275 upregulated lncRNAs and 209 downregulated lncRNAs were found between AD samples and control samples. The PPI network constructed consists of 1016 nodes and 13,946 edges. Ten hub genes were selected to identify target miRNAs and ceRNAs. On the basis of the ceRNA hypothesis, a circRNA/lncRNA-miRNA-mRNA network was established. It included five lncRNAs (TRHDE-AS1, SNHG10, OIP5-AS, LINC00926 and LINC00662), 26 circRNAs, five miRNAs (hsa-miR-3158-3p, hsa-miR-4435, hsa-let-7d-3p, hsa-miR-330-5p and hsa-miR-3605-3p), and ten mRNAs (*RPL11*, *RPL34*, *RPL21*, *RPL22*, *RPL6*, *RPL32*, *RPL24*, *RPL35*, *RPL31*, and *RPL35A*). *RPL35* and *RPL35A* were found to be significantly associated with AD pathology in tau and Aβ line AD models by the AlzData database. The study discovered the significance of several lncRNA-miRNA-mRNA axes and circRNA-miRNA-mRNA axes that included *RPL35A* and *RPL35*. **Conclusions**: ceRNAs were found to be important regulators in the development of AD and provide potential biological therapy targets for AD management.

Keywords: Alzheimer's disease; lncRNA; miRNA; mRNA; circRNA; ceRNA network

1. Introduction

More than 90% of human genes are transcriptional genes, but most of them do not encode proteins and are transcribed into non-coding RNAs (ncRNAs) [1]. NcRNAs are classified into two main types: housekeeping ncRNAs and regulatory ncRNAs. Regulatory ncRNAs include long ncRNAs (lncRNAs >200 nucleotides, nts), microRNAs (miRNAs, 21–23 nts), PIWI-Interacting RNA (piRNA, 25–33 nts) and circular RNAs (circRNAs) [2]. Regulatory ncRNAs interact with each other in a complex network to regulate both their abundance and gene expression [3].

Alzheimer's disease (AD) is considered to be a complex heterogeneous disease. Its exact pathogenesis remains unknown, and has no effective treatment method [4]. Thus, there is a need for further research on underlying disease processes to better understand AD and aid the development of feasible treatment options. Considerable evidence shows that ncRNAs, particularly lncRNAs, miRNAs, and circRNAs, are a major class of regulatory molecules involved in the pathophysiology associated with AD [5].

LncRNAs are ncRNAs with a length of more than 200 nts and have been reported as important for cell regulation. Cytoplasmic lncRNA act as miRNA sponges or miRNA precursors to alter the expression and function of miRNA. They also recognize target messenger RNA (mRNA) and interact with cellular translation mechanisms. In SH-SY5Y cells, the upregulation of nuclear enriched abundant transcript 1 (lncRNA NEAT1) has been related to the downregulation of miR-27a-3p and upregulation of amyloid (Aβ), β-amyloid-precursor-protein-cleaver-enzyme 1 (BACE1) protein, amyloid precursor protein (APP), and tau protein [6]. Studies suggest that LncRNA Ribonuclease P RNA

component H1 (Rpph1) participate in the regulation of the onset and progression of AD by competing with miR-330-5p and miR326-3p [7].

MiRNAs are small molecules with transcripts of 21–23 nts. Changes in the levels of several miRNAs and their targeted mRNA have been reported to affect the development and progression of the disease such as APP production, Tau aggregation, Aβ production, protein misfolding, neuroinflammation, and oxidative damage [8]. For example, compared with controls, the expression of miR-485-3p was significantly increased in the brain tissues of AD patients [9], and MiR-485-3p antisense oligonucleotide (ASO) reduced the expression level of Aβ via phagocytosis of Aβ mediated by CD36 [9]. Additionally, it is reported that miR-146a overexpression reduces cognitive impairment, secretion of proinflammatory cytokines, Aβ plaque accumulation and protects the neurons of APP/PS1 transgenic mice from damage [10].

CircRNAs are non-coding RNA molecules that do not have a 5′ end cap and a 3′ end poly (A) tail that form a ring structure by a covalent bond. CircRNAs have been reported to play a significant role in various biological functions as a miRNA sponge and transcription regulator. For example, circRNA_0003611 is augmented in AD patients. It was reported that silenced circRNA_0003611 might reduce neuronal damage triggered by Aβ via adjusting the miR-383-5p/kinesin family member 1B (KIF1B) axis [11]. CircRNA Cwc27 is a neuronal-rich circRNA substantially expressed in the brain and significantly increases in AD patients and mice [12]. CircRNA Cwc27 deficiency significantly ameliorates AD-related pathological features and increases cognitive function [12]. CircRNA Cwc27 was shown to directly bind to purine-rich element-binding protein A (Pur-α) and repress Pur-α recruitment to AD gene promoter clusters [13].

Competitive endogenous RNA (ceRNA) includes mRNA of coding-protein lncRNA and circRNA. Numerous studies have emphasized that these ceRNA molecules regulate miRNA target gene expression via competitively binding to the same miRNA by miRNA responsive elements (MREs). Recently, it was reported that the ceRNA network plays a critical role in many diseases, such as cardiovascular, neuroimmune and neurodegenerative disease [14–16]. Thus, the ceRNA network offers new approaches to understanding AD. Though some ceRNAs have been found related to AD progression, there is currently little discussion of the role of the ceRNA regulatory network in AD. In this study, data were obtained from the gene expression omnibus (GEO) database. Differentially expressed circRNAs (DEcircRNAs), mRNAs (DEmRNAs), lncRNAs (DElncRNAs), and miRNAs (DEmiRNAs) were screened from sequencing data. The targeted miRNAs and their related circRNAs and lncRNAs were forecast, an integrated ceRNA network was constructed, and their potential value for AD diagnosis was explored. The key pathways and regulatory mechanisms of central genes were analyzed and discussed using bioinformatics tools. MiRNAs, targeted mRNAs, related lncRNAs, and circRNAs involved in the ceRNA network may be possible biomarkers and treatment targets for AD. The workflow is shown in Fig. 1.

2. Materials and Methods

2.1 Microarray Datasets

MRNA, miRNA, circRNA, and lncRNA expression datasets were obtained from the GEO database (https://www.ncbi.nlm.nih.gov/geo/). GSE63063 was selected for analysis of differentially expressed mRNAs from AD patients compared with controls, in which 329 samples (145 AD cases and 104 controls) based on GPL6947 platform (chip A) were collected and 382 samples (139 AD cases and 134 controls) based on the GPL10558 platform (chip B) were selected. GSE120584 was downloaded to derive DEmiRNAs between AD patients and controls, in which 1309 data sets were downloaded (1021 AD cases and 288 controls) for analysis. The circRNA expression data were derived from GSE161435 (3 AD cases and 3 control cases). The lncRNAs expression data were obtained from GSE182910 (3 AD cases and 3 control cases).

Details of the microarray data selected are described in Table 1.

2.2 Identification of DEmRNAs, DEmiRNAs, DecircRNAs, and DElncRNAs

The differential expression analysis of mRNAs, miRNAs, circRNAs, and lncRNAs among different groups was performed using GEO2R. GEO2R completed the analysis using limma R software packages (version 3.56.0) (limma R software, University of Melbourne, Parkville, Victoria, Australia). $p < 0.05$, false discovery rate (FDR) <0.05 and an absolute value of $\log_2$-fold ≥ 0.01 were used as thresholds to screen DEmRNAs. mRNAs without symbol annotation were excluded. When different probes fitted the same mRNA, the mRNAs with the highest absolute value of $\log_2$-fold were selected.

The criteria for the selection of DEmiRNAs were FDR <0.05, $p < 0.05$ and the absolute value of $\log_2$-fold >0.2. The miRNA with the highest absolute value of $\log_2$-fold was selected when different probes fitted the same miRNA.

DEcircRNAs were identified with the criterion p-value < 0.05 and $\log_2$-fold >0.4 were considered significant.

DElncRNAs with $p < 0.05$ and $\log_2$-fold >1.5 were considered to indicate significant differences in expression.

2.3 Functional Enrichment Analysis for DEmRNAs

Kyoto Encyclopedia of Genes and Genomes (KEGG) and Gene Ontology (GO) enrichment analyses for the DEmRNAs were executed using the Metascape database (v3.5.20230501) (http://metascape.org/gp/index.html#/main/step1). Significant enrichment was selected with a threshold of $p < 0.05$.

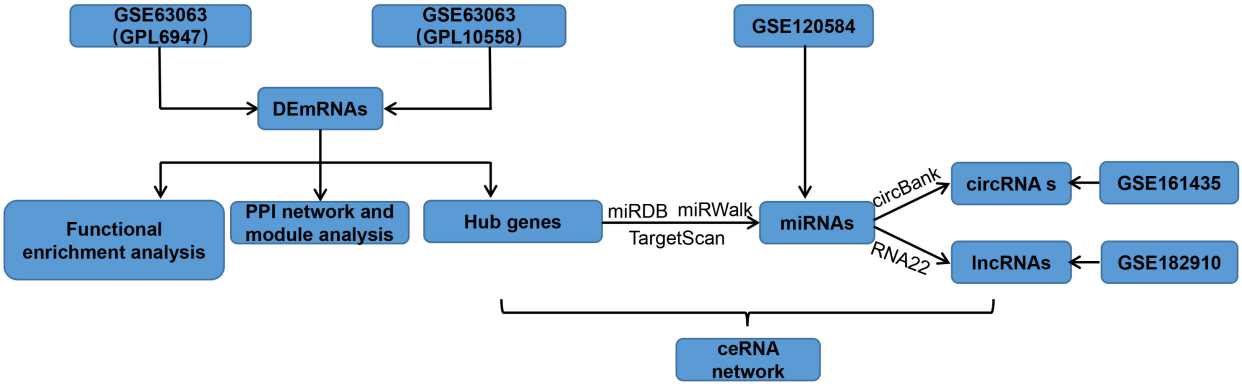

Fig. 1. Study design flowchart. DEmRNAs, differentially expressed mRNAs; miRNAs, microRNAs; circRNAs, circular RNAs; lncRNAs, long ncRNAs; PPI, protein-protein interaction; ceRNA, competitive endogenous RNA.

Table 1. The detail of selected microarray data.

GEO accession number	Sample size (AD/control)	Platform
mRNA		
GSE63063 (Blood)	AD = 145 HC = 104	GPL6947 Illumina HumanHT-12 V3.0 expression BeadChip
	AD = 139 HC = 134	GPL10558 Illumina HumanHT-12 V4.0 expression BeadChip
miRNA		
GSE120584 (Serum)	AD = 1021 HC = 288	GPL21263 3D-Gene Human miRNA V21_1.0.0
circRNA		
GSE161435 (Blood)	AD = 3 HC = 3	GPL21825 074301 Arraystar Human CircRNA microarray V2
lncRNA		
GSE182910 (Serum)	AD = 3 HC = 3	GPL21827 Agilent-079487 Arraystar Human LncRNA microarray V4 (Probe Name version)

AD, Alzheimer's disease; HC, control; GEO, gene expression omnibus; mRNA, messenger RNA.

2.4 PPI Network Integration of Modules and Their Analysis

The interaction relationships among DEmRNAs were constructed by STRING version 11.5 (https://cn.string-db.org/) [17]. High confidence (0.7) was selected as the cut-off criterion for the minimum required interaction score. The protein-protein interaction (PPI) network of DEmRNAs was visualized by Cytoscape 3.9.1 (Cytoscape, Institute for Systems Biology, Seattle, WA, USA) [18]. Key modules of the PPI network were screened using the Molecular Complex Detection (MCODE) plugin in Cytoscape 3.9.1 (Cytoscape, Institute for Systems Biology, Seattle, WA, USA). Cutoff = 2, node score cutoff = 0.2, k-core = 2, and maximum depth = 100 were regarded as selection criteria.

Additionally, the KEGG pathway enrichment of mRNAs in the significant modules was analyzed by Metascape database (v3.5.20230501) (http://metascape.org/gp/index.html#/main/step1). A $p < 0.05$ was considered significant.

2.5 Identification and Verification of Hub Genes

Hub genes of the network were identified by applying CytoHubba which is a plugin for Cytoscape 3.9.1 (Cytoscape, Institute for Systems Biology) [19]. The top ten nodes ranked by the maximum group centrality (MCC) algorithm were selected as hub genes. The AlzData database, a one-stop database, covers high-throughput omics data and high-confident functional data of AD [20]. The hub genes identified in this study were inserted into the AlzData database (http://www.alzdata.org/) to obtain each hub gene-related cell type and correlation with AD pathology (Aβ and tau). KEGG pathway enrichment of the hub genes was analysed via Metascape database (v3.5.20230501) (http://metascape.org/gp/index.html#/main/step1).

2.6 Screening of DEmiRNAs Target Hub Genes

Regulatory interaction between miRNAs and the hub genes was predicted by TargetScan (https://www.targetscan.org/vert_72/) [21], miRWalk (http://mirwalk.umm.uni-h

eidelberg.de/) [22], and miRDB (http://www.mirdb.org/) [22]. The DEmiRNAs that were potential targets of these hub genes were screened and a DEmiRNAs-hub genes network was constructed.

2.7 CeRNA Network of DEmiRNA, Hub Genes, DElncRNA, and DEcircRNA

A ceRNA network was constructed based on the regulatory mechanism among DEcircRNAs, DElncRNAs, DEmiRNAs, and DEmRNAs.

DEmiRNA binding sites of the circRNA were predicted via the circBank database (http://www.circbank.cn/) and RNA22 database was selected to calculate DEmiRNAs binding sites of the lncRNAs. Finally, a ceRNA network of hub genes, DEmiRNAs, DElncRNAs, and DEcircRNAs was constructed.

2.8 Statistical Analysis

Statistical analyses were performed using GraphPad Prism 8 (GraphPad Software, Inc., San Diego, CA, USA). A p-value < 0.05 was considered statistically significant. The differential expression of mRNAs and miRNAs was analyzed using limma R packages (version 3.56.0) (limma R software, University of Melbourne, Parkville, Victoria, Australia). A p-value < 0.05 and FDR <0.05 were considered statistically significant. Differential analyses of lncRNAs and circRNAs expression were performed using limma R packages (version 3.56.0) (limma R software, University of Melbourne). A p-value < 0.05 was considered statistically significant.

3. Results

3.1 Identification of DEmRNAs, DEmiRNAs, DEcircRNA, and DElncRNA

According to the parameters, 3051 DEmRNAs were identified from the GSE63063 datasets based on a GPL6947 platform (Fig. 2A), including 1618 upregulated and 1433 downregulated mRNAs. A total of 1961 DEmRNAs were obtained from the GSE63063 datasets based on the GPL10558 platform, containing 1056 upregulated and 905 downregulated mRNAs (Fig. 2B). Overlapping DEmRNAs of the two datasets were then screened. The outcome showed 711 common downregulated mRNAs (Fig. 2D), while 670 upregulated mRNAs were shared (Fig. 2E) (**Supplementary Table 1**).

A total of 372 DEmiRNAs were obtained from the GSE120584 datasets (Fig. 2C), 32 of which were downregulated and 340 were upregulated (**Supplementary Table 2**). Among them, the top five upregulated DEmiRNAs included hsa-miR-208a-5p, hsa-miR-6761-3p, hsa-miR-3646, hsa-miR-595, and hsa-miR-6754-3p, while the top five downregulated DEmiRNAs included hsa-miR-125a-3p, hsa-miR-6131, hsa-miR-24-3p, hsa-miR-125b-1-3p, and hsa-miR-22-3p.

There were 283 DEcircRNAs screened from the GSE161435 datasets, containing 78 upregulated and 205 downregulated circRNAs (**Supplementary Table 3**). The top five upregulated DEcircRNAs included hsa_circRNA_044837, hsa_circRNA_101213, hsa_circRNA_406841, hsa_circRNA_092388, and hsa_circRNA_104193, while the top five downregulated DEcircRNAs included hsa_circRNA_0102552, hsa_circRNA_0050212, hsa_circRNA_0102457, hsa_circRNA_0102551, and hsa_circRNA_0002532.

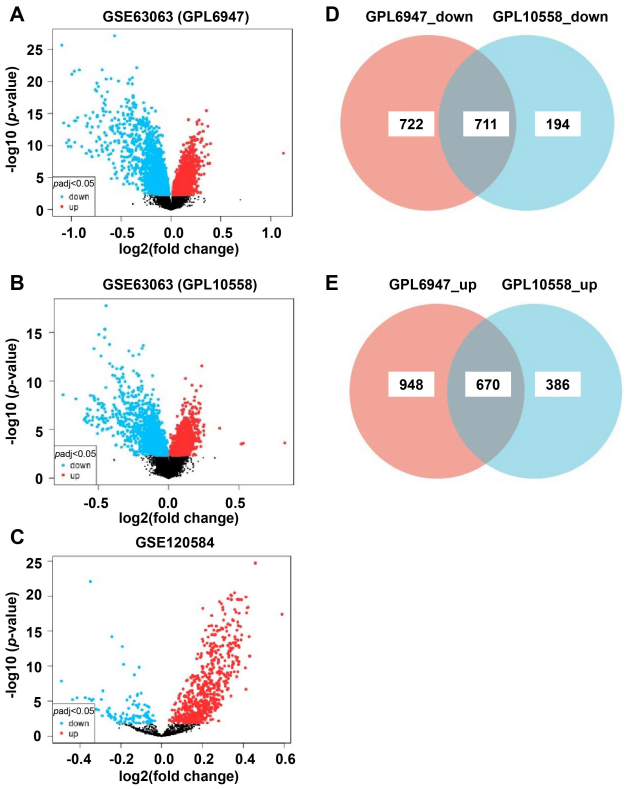

Fig. 2. Identification of DEmRNAs and DEmiRNAs. (A) Volcano plot of the GSE63063 (GPL6974) datasets. (B) Volcano plot of the GSE63063 (GPL10558) datasets. (C) Volcano plot of GSE120584 datasets. (D,E) Venn diagram of overlapping upregulated and downregulated DEmRNAs. DEmiRNAs, differentially expressed miRNAs; DEmRNAs, differentially expressed mRNAs.

A total of 484 DElncRNAs were found, including 275 upregulated and 209 downregulated lncRNAs. These DElncRNAs are shown in **Supplementary Table 4**. Among them, the top five upregulated DElncRNAs included G0S2, SLED1, LINC02065, TAGLN, and AC011193.1, while the top five downregulated DElncRNAs included MYOM2, AL935212.1, AC245452.5, LINC00989, and AL023693.1.

3.2 Functional Enrichment Analysis of DEmRNAs

Functional enrichment analysis showed that the upregulated DEmRNAs were mainly enriched in the regulation of response to biotic stimulus, regulation of defense response and regulation of innate immune response in the biological process (BP) category; secretory granule mem-

brane, tertiary granule, specific granule and specific granule membrane in the cellular component (CC) category; GTPase regulator activity, nucleoside-triphosphatase regulator activity, enzyme activator activity, and small GTPase activator activity in the molecular function (MF) category (Fig. 3A,C,E and **Supplementary Table 5**). For the downregulated DEmRNAs, functional enrichment analysis indicated that the enriched GO terms mainly included translation, peptide biosynthetic process, and peptide metabolic process in the BP category; ribosomal subunit, focal adhesion, cell-substrate junction, and mitochondrial protein-containing complex in the CC category; structural constituent of ribosome, rRNA binding, oxidoreduction-driven active transmembrane transporter activity and nicotinamide adenine dinucleotide (NADH) dehydrogenase (ubiquinone) activity in the MF category (Fig. 3B,D,F and **Supplementary Table 6**).

As shown in Fig. 3G,H and **Supplementary Tables 7,8**, KEGG pathways for the upregulated DEmRNAs mainly included osteoclast differentiation, NOD-like receptor signaling pathway, lipid and atherosclerosis and epstein-Barr virus infection (**Supplementary Table 7**), while the downregulated DEmRNAs were mainly enriched in various metabolic pathways such as ribosome, oxidative phosphorylation and Alzheimer disease (**Supplementary Table 8**).

3.3 Construction of PPI Interaction Network, Module Analysis, and Identification of Hub Genes

A PPI network was constructed, which consisted of 1016 nodes and 13,946 edges. The MCODE plug-in was utilized for finding key subnetworks and genes based on the relationship between edges and nodes in the network for downstream analysis. Based on MCODE analysis, 44 modules were obtained (**Supplementary Table 9**), 6 modules of which were selected for Fig. 4A–F. The highest score of module 1 is 53.724, which was significantly enriched in ribosomes and protein export (Fig. 4G). Module 2 was mainly related to the ribosome (Fig. 4H). Similarly, module 3 was significantly enriched in oxidative phosphorylation, and so on (Fig. 4I). Module 4 was mainly assembled in ribosome biogenesis (Fig. 4J). Module 5 was primarily associated with the proteasome (Fig. 4K). Module 6 was mainly associated with the spliceosome (Fig. 4L).

Based on importance, ten downregulated genes in module 1 were considered as hub genes of the network, such as ribosomal protein L11 (*RPL11*), ribosomal protein L34 (*RPL34*), ribosomal protein L21 (*RPL21*), ribosomal protein L22 (*RPL22*), ribosomal protein 61 (*RPL6*), ribosomal protein L32 (*RPL32*), ribosomal protein L24 (*RPL24*), ribosomal protein L35 (*RPL35*), ribosomal protein L31 (*RPL31*), and ribosomal protein L35A (*RPL35A*). These hub genes are primarily enriched in ribosomes (Table 2 and Fig. 5A,B). Moreover, the AlzData database was utilized for analysing the hub genes. Nine of these hub genes (*RPL11*, *RPL34*, *RPL22*, *RPL6*, *RPL32*, *RPL24*, *RPL35*, *RPL31*, and *RPL35A*) were confirmed to be significantly expressed in various parts of the brain based on the results (Fig. 5C–K). The hub genes related to AD were ranked using the AlzData database (Table 3). According to the score of convergent functional genomics (CFG), *RPL35*, *RPL24*, *RPL22*, and *RPL35A* were identified as significantly relevant to pathology of AD mouse models of Aβ type. In AD mouse models of the tau line, *RPL35*, *RPL31*, *RPL35A*, and *RPL21* were significantly related to AD pathology.

Based on these results, it was shown that these hub genes may have a significant role in AD pathogenesis.

Table 2. The top ten genes listed as hub genes through the maximum group centrality (MCC) algorithm.

Gene name	Score	Expression
RPL35	3.62661×10^{53}	downregulated
RPL31	3.62661×10^{53}	downregulated
RPL24	3.62661×10^{53}	downregulated
RPL34	3.62661×10^{53}	downregulated
RPL32	3.62661×10^{53}	downregulated
RPL11	3.62661×10^{53}	downregulated
RPL22	3.62661×10^{53}	downregulated
RPL35A	3.62661×10^{53}	downregulated
RPL6	3.62661×10^{53}	downregulated
RPL21	3.62661×10^{53}	downregulated

3.4 The DEmiRNAs-Hub Gene Network

MiRNAs are endogenous non-coding RNAs with regulatory functions. The size of miRNAs is about 21~23 nts. They inhibit target mRNA expression by recognizing target mRNA through base complementary pairing. Based on this, the DEmiRNAs-hub genes pairs with an up-down mode were selected for further study.

A total of 337 overlapped upregulated DEmiRNAs related to the above ten downregulated hub genes were collected using TargetScan, miRWalk, and miRDB databases. Based on the regulatory relationship, a miRNA-mRNA network was constructed, as given in **Supplementary Table 10**.

To further verify the 337 overlapped upregulated DEmiRNAs, a GSE46579 dataset for studying miRNA expression profiles in the blood of AD patients and controls was collected. In total, GSE46579 detected 180 differentially expressed miRNAs, including 90 downregulated and 90 upregulated miRNAs in AD samples compared with controls. Then, the common DEmiRNAs were screened between the 337 DEmiRNAs and the 180 differentially expressed miRNAs, which revealed 5 common upregulated DEmiRNAs. Information in detail is shown in Table 4.

3.5 CeRNA Network of DEmiRNAs, Hub Genes, DElncRNAs, and DEcircRNAs

In addition to mRNA, lncRNA and circRNA also have MREs. When lncRNA or circRNA and mRNA have the

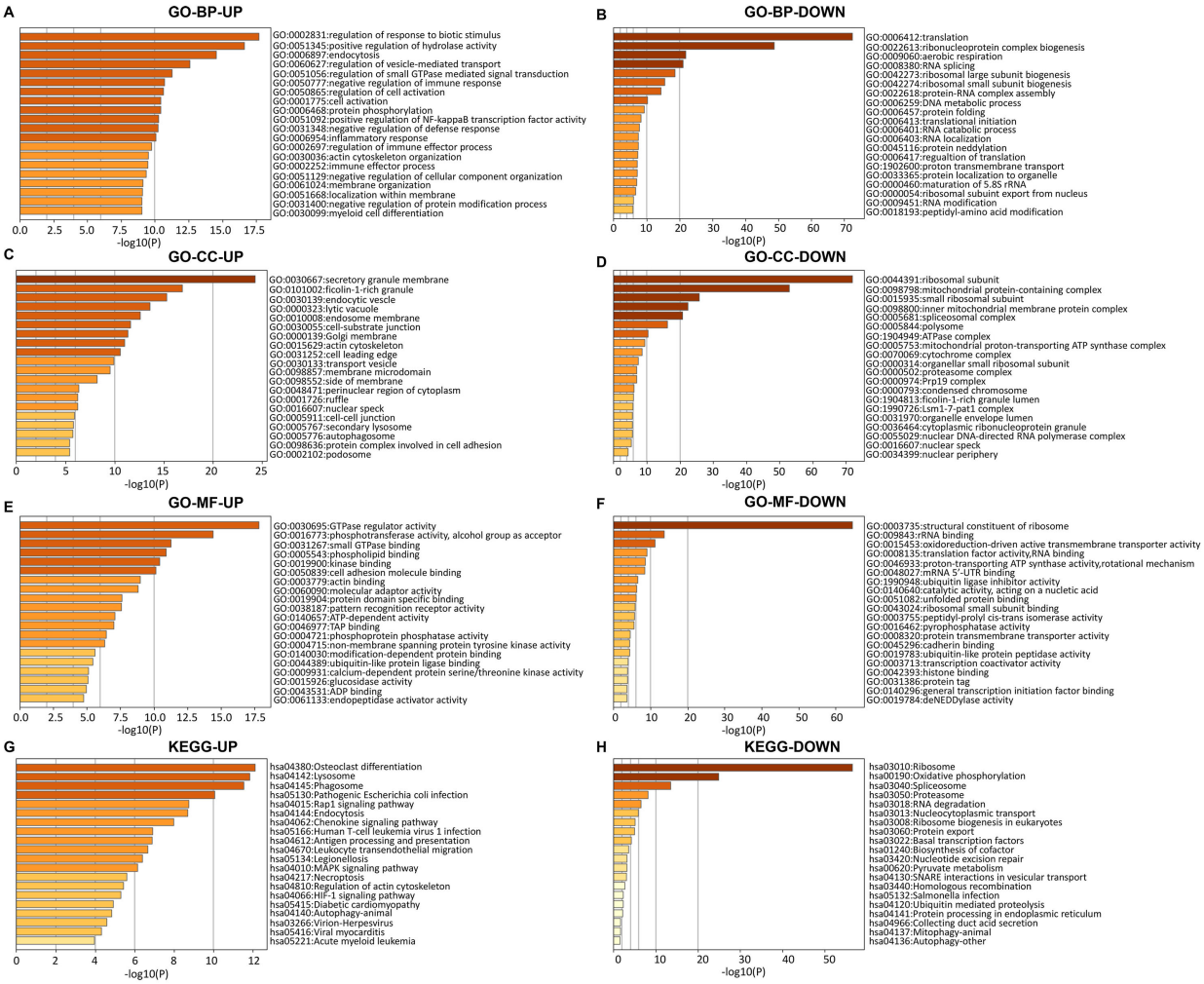

Fig. 3. Enrichment analysis of function for upregulated and downregulated differentially expressed mRNAs (DEmRNAs). Enrichment analysis of the biological process (BP) for DEmRNAs (A,B), Enrichment analysis of cellular component (CC) for DEmRNAs (C,D), and enrichment analysis of molecular function (MF) for DEmRNAs (E,F). (G,H) KEGG analysis for DEmRNAs. UP, upregulated; DOWN, downregulated; FDR, false discovery rate; KEGG, Kyoto Encyclopedia of Genes and Genomes; GO, Gene Ontology.

Table 3. Ranking of convergent functional genomic (CFG) of target genes.

Gene	eQTL	GWAS	PPI	Early_DEG	Pathology correlation (Aβ)	Pathology correlation (tau)	CFG
RPL35	2	0	PSEN1	NA	0.485, ***	0.763, ***	3
RPL31	NA	0	PSEN1	yes	0.273, ns	0.621, *	3
RPL24	0	0	-	yes	0.368, *	0.508, ns	2
RPL34	0	0	PSEN1	NA	NA	NA	1
RPL32	2	0	PSEN1	NA	NA	NA	2
RPL11	1	0	-	NA	NA	NA	1
RPL22	2	0	-	yes	0.370, *	0.400, ns	3
RPL35A	1	0	-	yes	0.339, *	0.546, *	3
RPL6	1	1	-	NA	NA	NA	2
RPL21	0	0	-	NA	0.278, ns	0.566, *	1

Note: eQTL: target gene expression is affected by variation of the AD gene ($p < 1^{-3}$). GWAS: $p < 1^{-3}$. PPI: interaction between target genes and APP, PSEN1, PSEN2, APOE, or MAPT is significant ($p < 0.05$); Early_DEG: differential expression of target gene in AD mouse models before the onset of AD pathology; Pathology correlation (Aβ): correlation between expression of target gene and AD pathobiology in AD mouse models of Aβ line; Pathology correlation (tau): correlation between expression of target gene and AD pathobiology in AD mouse models of tau line. ns, Non-significant; * $p < 0.05$; *** $p < 0.001$; CFG: total CFG score of target gene. CFG score is increased based on the importance of the above evidence.

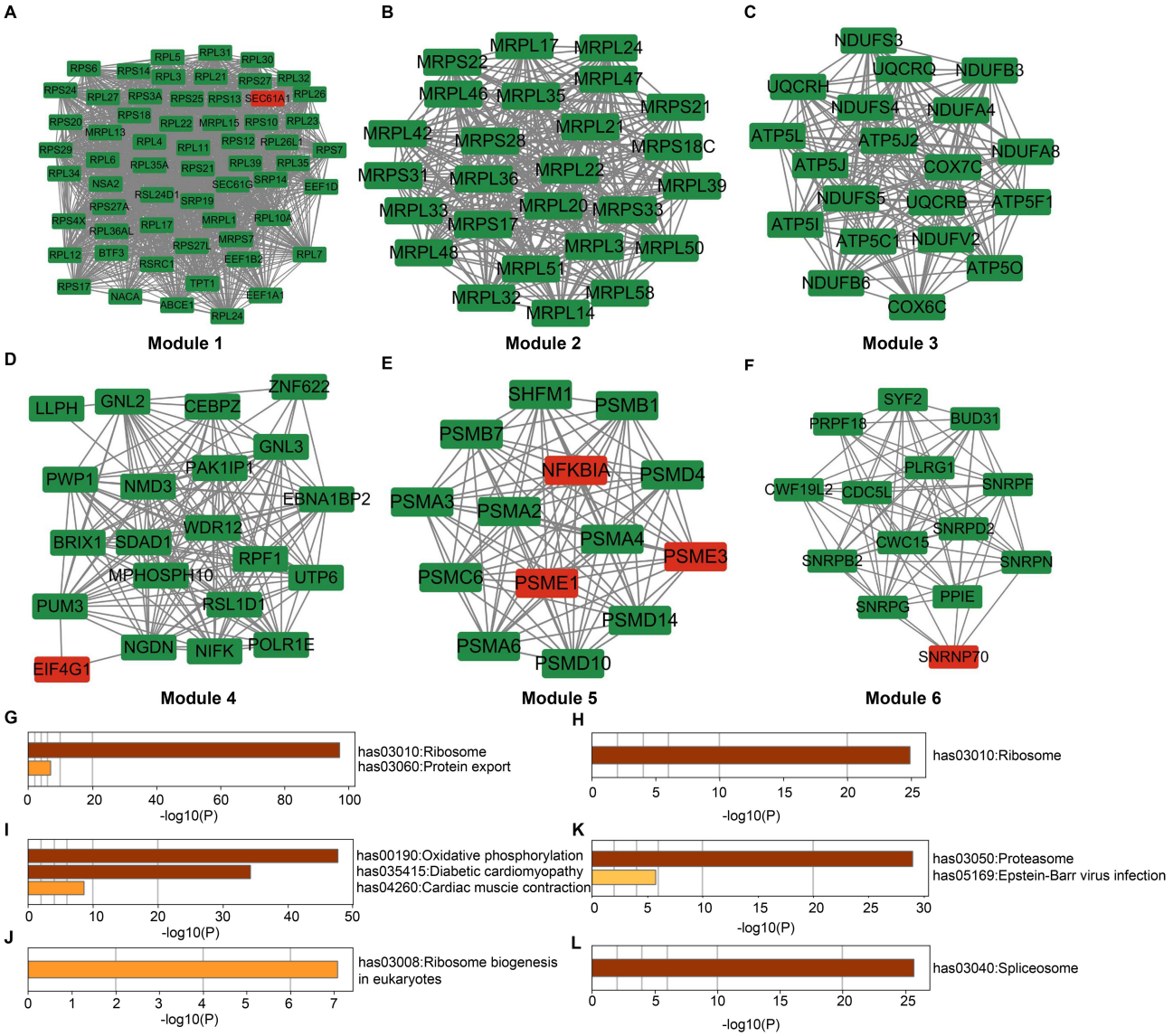

Fig. 4. Construction of the PPI network and analysis of modules. (A–F) PPI network of for the selected 6 modules. Red: Upregulated DEmRNAs. Green: Downregulated DEmRNAs. (G–L) Enrichment of KEGG pathway of these modules. DEmRNAs, differentially expressed mRNAs; KEGG, Kyoto Encyclopedia of Genes and Genomes.

Table 4. Common upregulated DEmiRNAs in GSE46579 and the 337 overlapped upregulated DEmiRNAs.

miRNA symbol	GSE120584			GSE46579		
	adj. *p*-value	*p*-value	logFC	adj. *p*-value	*p*-value	logFC
has-miR-3158-3p	0.000000547	5.09×10^{-8}	0.277258	0.027374587	0.008323958	0.501717096
has-miR-4435	0.00000203	0.000000211	0.412811	0.01527147	0.004076448	0.648281094
has-let-7d-3p	0.00063	0.000109	0.213241	0.026760404	0.007878648	1.069946327
has-miR-330-5p	0.0000441	0.0000058	0.252895	0.000771818	0.000119924	1.007092612
has-miR-3605-3p	5.01×10^{-10}	2.56×10^{-11}	0.348935	0.048411001	0.0164906	0.832622225

same MREs, they will competitively bind to the same miRNAs. In other words, lncRNA or circRNA expression level in cells directly influences the expression of miRNAs that bind to the corresponding mRNA. That is, through the MREs bridge, lncRNA or circRNA indirectly regulating the mRNA expression level, thus regulate cell function.

On the basis of the aforementioned 5 overlapped upregulated DEmiRNAs, 36 DElncRNA-DEmiRNA regulatory pairs were obtained using RNA22 and 53 DEcircRNA-DEmiRNA regulatory pairs were obtained using CircBank. Based on the ceRNA hypothesis, the DEcircRNAs/DElncRNAs-DEmiRNAs-hub genes

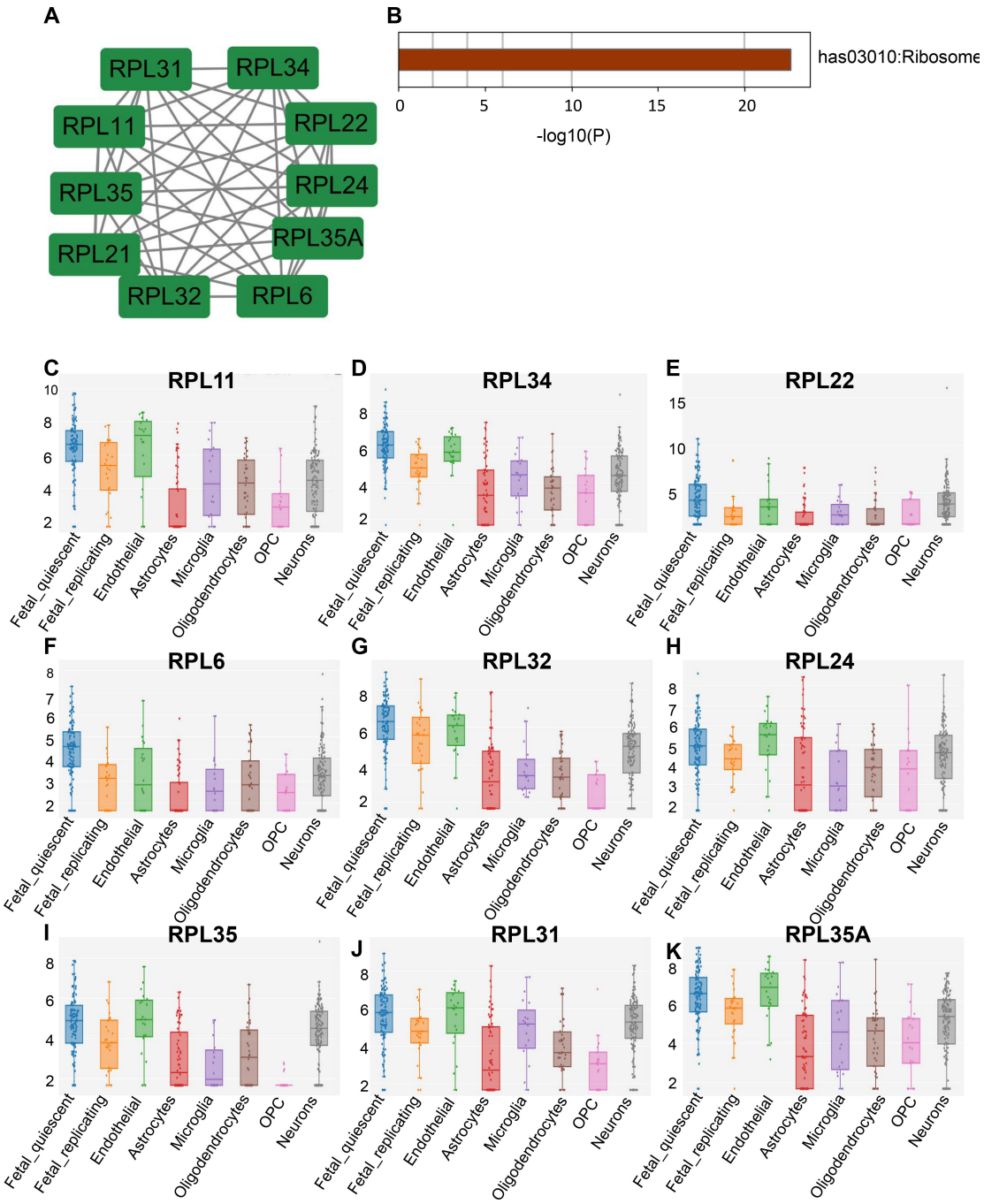

Fig. 5. Verification of hub genes. (A) Regulatory network of the hub genes. (B) KEGG pathway enrichment of hub genes. (C–K) Hub gene expression in different parts of the brain.

with a mode of down-up-down were chosen for further investigation.

A DEcircRNAs-DEmiRNAs-hub genes network was constructed by Cytoscape 3.9.1 and included 26 circRNAs, 5 miRNAs, and 10 mRNAs (Table 5 and Fig. 6).

Generally, the lncRNAs in cytoplasm competitively bound to miRNA to regulate mRNA expression level. The RNALocate v2.0 database was selected to perform the intracellular localization of these lncRNAs (Fig. 7). It should be noted that the lncRNAs not located in cytoplasm or unclear were excluded from the network. The network of DElncRNAs-DEmiRNAs-hub genes (including 5 lncRNAs, 3 miRNAs and 10 mRNAs) is given in Table 6 and Fig. 8. AD-associated lncRNAs were then identified from the 5 DElncRNAs using the LncRNADisease v2.0 online

software. Out of the 5 DElncRNAs, 3 have previously been shown to be associated with AD (SNHG10, OIP5-AS1 and LINC00662).

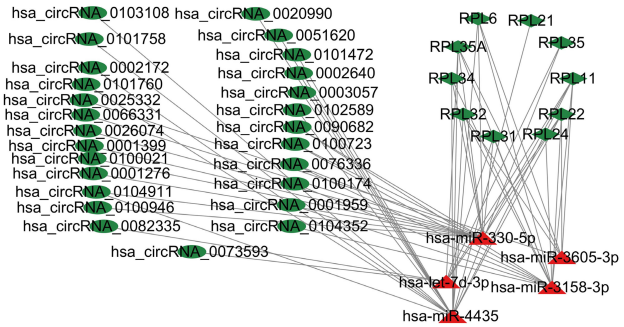

Fig. 6. The circRNAs-miRNAs-mRNAs network. Triangle nodes indicate miRNAs, ellipse-shaped nodes indicate circRNAs and diamond nodes indicate hub genes. Red: upregulated nodes. Green: downregulated nodes.

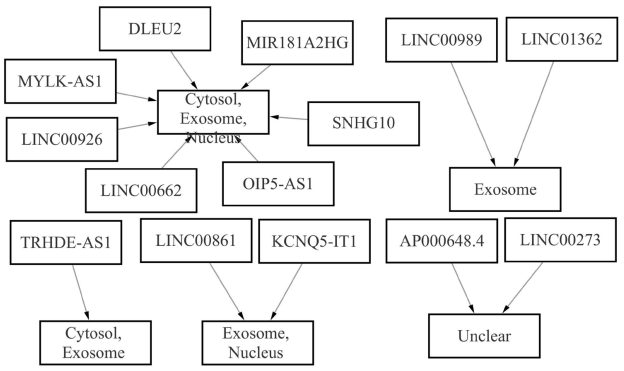

Fig. 7. Intracellular localization of lncRNAs.

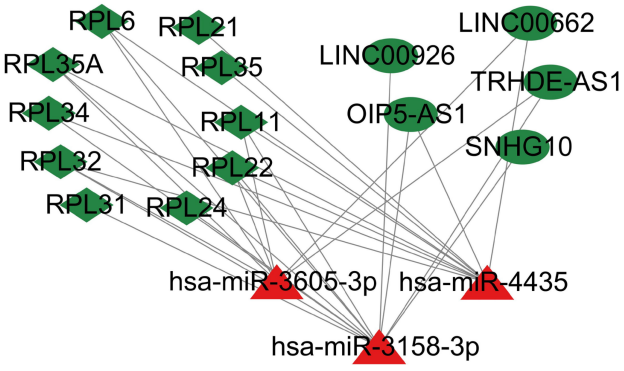

Fig. 8. The lncRNAs-miRNAs-mRNAs network. Triangle nodes: miRNAs, ellipse-shaped nodes: lncRNAs, and diamond nodes: hub genes. Red: Upregulated nodes. Green: Downregulated nodes.

4. Discussion

Various ceRNAs are abnormally expressed in AD [23–25] and mounting evidence has shown the relationships among dysregulated lncRNAs, circRNAs, miRNAs, and mRNAs and the construction of AD-related ceRNA networks [26]. The ceRNA network is beneficial for a deeper understanding of the AD mechanism. In this study, transcriptome data of AD patients from the GEO database was used that contained mRNAs, circRNA, lncRNAs, and miRNAs. A total of 1381 DEmRNAs, 283 DEcircRNA, 484 DElncRNAs, and 372 DEmiRNAs were identified. A circRNA/lncRNA-miRNA-mRNA ceRNA network with biologic functions in AD was constructed following bioinformatic analysis. It is noteworthy that the ceRNA hypothesis indicates that there is a negative correlation between the ceRNA and miRNA expression levels but a positive correlation with mRNA expression. Therefore, the predicted relationships were integrated with the corresponding expression data to obtain more reliable results.

Through functional enrichment analysis, the upregulated DEmRNAs were mainly associated with regulation of response to biotic stimulus, regulation of defense response and regulation of innate immune response. Additionally, the downregulated DEmRNAs were mainly involved in translation, peptide biosynthetic process and peptide metabolic process. Importantly, ten hub genes were identified (*RPL11*, *RPL34*, *RPL21*, *RPL22*, *RPL6*, *RPL32*, *RPL24*, *RPL35*, *RPL31* and *RPL35A*) using the CytoHubba tool. These ten hub genes were found to be downregulated in AD samples. The results of enrichment analysis showed that hub genes were mainly involved in ribosomes. These hub genes are members of a ribosomal protein family, which is important for the end and correctness of translation in the ribosome [27]. Ribosomal proteins were reported to be significant parts of ribosomes and participate in regulating bioprocesses [28]. Recently, it was reported that ribosomal proteins are tightly related to the progress of AD [29–31].

Previous investigation has shown that the low expression level of *RPL11* is related to ribosome pathway dysfunction during AD development, which is the same as the conclusion of this analysis. There was evidence to suggest that *RPL11* was correlated with brain maturation [32]. *RPL11* contributed to the cortical neuron function damaged by ribosomal stress in neurodegenerative diseases [33]. Thus, it was speculated here that *RPL11* may influence AD progression via the ribosome pathway. RPL34, a member of the ribosomal protein L34E family, is a highly conserved protein and has been demonstrated to participate in the occurrence and development of human malignancies. No evidence showed a role for *RPL34* in AD development. The *RPL21* gene was identified to be involved in Parkinson's disease [34]. *RPL22*, a ribosomal protein, is induced by Cre recombinase, which primarily participates in the formation of the 60S subunit [35]. Recent research has demonstrated

Table 5. Regulatory relationship of DEcircRNAs-DEmiRNAs-hub genes with a down-up-down mode.

DEmiRNAs	circRNAs associated with miRNAs	Targeted hub genes of DEmiRNAs
has-miR-3158-3p (upregulated)	has_circRNA_0090682 (down), has_circRNA_0100723 (down), has_circRNA_0076336 (down), has_circRNA_0100174 (down), has_circRNA_0001959 (down), has_circRNA_0104352 (down)	*RPL11* (down), *RPL22* (down), *RPL24* (down), *RPL31* (down), *RPL32* (down), *RPL34* (down), *RPL35A* (down), *RPL6* (down)
has-miR-4435 (upregulated)	has_circRNA_0101760 (down), has_circRNA_0002172 (down), has_circRNA_0101758 (down), has_circRNA_0103108 (down), has_circRNA_0020990 (down), has_circRNA_0051620 (down), has_circRNA_0101472 (down), has_circRNA_0002640 (down), has_circRNA_0003057 (down), has_circRNA_0102589 (down), has_circRNA_0104911 (down)	*RPL11* (down), *RPL21* (down), *RPL22* (down), *RPL32* (down), *RPL34* (down), *RPL35* (down), *RPL35A* (down), *RPL6* (down)
hsa-let-7d-3p (upregulated)	hsa_circRNA_0073593 (down), hsa_circRNA_0082335 (down)	*RPL11* (down), *RPL22* (down), *RPL31* (down), *RPL35* (down), *RPL35A* (down)
hsa-miR-330-5p (upregulated)	hsa_circRNA_0090682 (down), hsa_circRNA_0100946 (down), hsa_circRNA_0104911 (down), hsa_circRNA_0001276 (down), hsa_circRNA_0100021 (down), hsa_circRNA_0001399 (down), hsa_circRNA_0026074 (down), hsa_circRNA_0066331 (down), hsa_circRNA_0076336 (down), hsa_circRNA_0100723 (down)	*RPL11* (down), *RPL22* (down), *RPL31* (down), *RPL32* (down), *RPL34* (down), *RPL35A* (down), *RPL6* (down)
hsa-miR-3605-3p (upregulated)	hsa_circRNA_0025332 (down)	*RPL11* (down), *RPL22* (down), *RPL32* (down), *RPL35A* (down), *RPL6* (down)

Table 6. Regulatory relationship of DElncRNAs-DEmiRNAs-hub genes with a down-up-down mode.

DEmiRNAs	lncRNAs associated with miRNAs	Targeted hub genes of DEmiRNAs
hsa-miR-3158-3p (upregulated)	TRHDE-AS1 (down), SNHG10 (down)*, OIP5-AS1 (down)*, LINC00926 (down)	*RPL11* (down), *RPL22* (down), *RPL24* (down), *RPL31* (down), *RPL32* (down), *RPL34* (down), *RPL35A* (down), *RPL6* (down)
hsa-miR-4435 (upregulated)	OIP5-AS1 (down)*, LINC00662 (down)*	*RPL11* (down), *RPL21* (down), *RPL22* (down), *RPL32* (down), *RPL34* (down), *RPL35* (down), *RPL35A* (down), *RPL6* (down)
hsa-miR-3605-3p (upregulated)	TRHDE-AS1 (down), LINC00662 (down)*	*RPL11* (down), *RPL22* (down), *RPL32* (down), *RPL35A* (down), *RPL6* (down)

* Previously known to be associated with Alzheimer's disease.

that *RPL22* plays a significant role in normal T cell development to arrest new protein synthesis by regulating endoplasmic reticulum stress signal transduction [36] and deactivation or deficiency of the single allele of *RPL22* has been found [37]. However, its association with neurodegenerative diseases such as AD has not been evaluated. *RPL6* is a gene encoding a 60S subribosome, which plays an important role in oxidative phosphorylation and neuronal signal transduction in neurodegenerative diseases such as Parkinson's disease [38]. *RPL6* has been reported to be down-regulated in Parkinson's disease and induce 5′-adenosine monophosphate (AMP)-activated protein kinase signaling activation [39]. Similarly, down-regulation of *RPL6* was observed in Parkinson's disease peripheral blood mononuclear cell samples [40]. However, its function in AD is unclear. Knockdown of *RPL32* significantly represses hepatocellular carcinoma proliferation [41]. *RPL24* is another translation factor related to tumorigenesis. *RPL24* reduction was found to be associated with over-expression of p53, suggesting that *RPL24* in tumorigenesis is p53 dependent [42]. *RPL35* encodes a protein of the 60s ribosomal subunit, which is part of the ribosomal protein L29 family. The L29 family proteins have been found to be usually related to the activation of oncogenes and tumor suppressor genes. However, little study of *RPL35* function on neurodegenerative disease development has been found [43,44]. *RPL31*, a 60S large ribosomal subunit protein, was demonstrated to be correlated with the cell cycle and regulate cancer development and progression via the p53 pathway [45]. Prior literature has shown that *RPL35A* was the first to be involved in Diamond-Blackfan anemia, which was found to act as a biomarker in tumor angiogenesis [46]. *RPL35A*

has also been reported to be a significant down-regulator in an APP/PS1 mouse model of AD [47]. However, little is known about the relationship between *RPL35A* and AD development.

Three upregulated miRNAs (hsa-miR-3158-3p, hsa-miR-4435, and hsa-miR-3605-3p) were screened from AD samples in this ceRNA network. Among them, previous research has reported the upregulation of hsa-miR-4435 in AD samples [48]. This study was consistent with what is reported here. Additionally, the relationship of hsa-miR-3158-3p and hsa-miR-3605-3p with the pathogenesis of AD has not previously been reported. Similarly, five downregulated lncRNAs (TRHDE-AS1, SNHG10, OIP5-AS, LINC00926, and LINC00662) were found in AD samples. Three of them (SNHG10, OIP5-AS, and LINC00662) have been found to be correlated to the progression of AD by LncRNADisease v2.0. LINC00662 is a newly discovered long noncoding RNA. Previous study has shown that LINC00662 knockdown lowers the permeability of the blood brain barrier in the AD microenvironment due to enhanced tight junction-related protein expression levels [49]. Moreover, the ceRNA network constructed here predicted 26 differentially expressed circRNAs (see Table 4) that have been identified to be downregulated in AD. Among them, circRNA_0051620 was found to facilitate the occurrence and development of gastric cancer via acting as a miR-338-3p sponge and inhibiting ADAM17 [50]. However, there is little research on other circRNAs.

Notably, this study identified the clinical significance of several lncRNA-miRNA-mRNA and circRNA-miRNA-mRNA axes that included *RPL35A* and *RPL35*. LncRNA SNHG10 and OIP5-AS1 might be helpful for the development of AD via acting as a hsa-miR-3158-3p sponge and inhibiting the target mRNA *RPL35A* expression level. LncRNA LINC00662 might help the development of AD via acting as a sponge of hsa-miR-3605-3p and inhibiting the target mRNA *RPL35A* expression level. LncRNA OIP5-AS1 and LINC00662 might be helpful in the development of AD via acting as a sponge of hsa-miR-4435 and regulating target mRNA *RPL35* expression level. Six differentially expressed circRNAs (hsa_circRNA_0090682, hsa_circRNA_0100723, hsa_circRNA_0076336, hsa_circRNA_0100174, hsa_circRNA_0001959, and hsa_circRNA_0104352) might regulate the development of AD via acting as a sponge of hsa-miR-3158-3p and inhibiting the target mRNA *RPL35A* expression. 11 circRNAs with differential expression (hsa_circRNA_0101760, hsa_circRNA_0002172, hsa_circRNA_0101758, hsa_circRNA_0103108, hsa_circRNA_0020990, hsa_circRNA_0051620, hsa_circRNA_0101472, hsa_circRNA_0002640, hsa_circRNA_0003057, hsa_circRNA_0102589, and hsa_circRNA_0104911) might regulate the development of AD via acting as a sponge of hsa-miR-4435 and inhibiting the expression level of target mRNA *RPL35A* and *RPL35*. Two circRNAs with differential expression (hsa_circRNA_0073593 and hsa_circRNA_0082335) might regulate the development of AD by sponging hsa-let-7d-3p and inhibiting the target mRNA *RPL35A* and *RPL35* expression level. Ten differentially expressed circRNAs (hsa_circRNA_0090682, hsa_circRNA_0100946, hsa_circRNA_0104911, hsa_circRNA_0001276, hsa_circRNA_0100021, hsa_circRNA_0001399, hsa_circRNA_0026074, hsa_circRNA_0066331, hsa_circRNA_0076336, and hsa_circRNA_0100723) were found to be correlated to AD development via acting as a sponge of hsa-miR-330-5p and inhibiting the expression level of the target mRNA *RPL35A*. Hsa_circRNA_0025332 was found to be related to AD progression via acting as a sponge of hsa-miR-3605-3p and inhibiting the target mRNA *RPL35A* expression. Additionally, this analysis using the AlzData database showed that the target mRNA *RPL35* and *RPL35A* were significantly associated with the clinicopathological features of AD. This study could provide new insights for understanding the interaction of ceRNA regulation and the pathogenesis of AD.

5. Conclusions

1381 differentially expressed overlapping mRNAs (711 downregulated and 670 upregulated) were identified between AD samples and control samples. 372 differentially expressed miRNAs (32 downregulated and 340 upregulated miRNAs) were obtained from AD samples compared with control samples. A total of 283 differentially expressed circRNAs (upregulation of 78 circRNAs and downregulation of 205 circRNAs) were screened. 275 upregulated lncRNAs and 209 downregulated lncRNAs were found between AD samples and control samples. Based on the ceRNA hypothesis, networks were constructed for lncRNA-miRNA-mRNA and circRNA-miRNA-mRNA, which include five lncRNAs (TRHDE-AS1, SNHG10, OIP5-AS, LINC00926 and LINC00662), 26 circRNAs, five miRNAs (hsa-miR-3158-3p, hsa-miR-4435, hsa-let-7d-3p, hsa-miR-330-5p and hsa-miR-3605-3p), and ten mRNAs (*RPL11*, *RPL34*, *RPL21*, *RPL22*, *RPL6*, *RPL32*, *RPL24*, *RPL35*, *RPL31* and *RPL35A*). Based on the important role of *RPL35* and *RPL35A* in AD reported in the AlzData database, the significance of the ceRNA network that includes *RPL35A* and *RPL35* was discovered. These ceRNA networks are believed to be involved in the development of AD.

Availability of Data and Materials

All the data supporting the results of this study are included in the manuscript and the Supplementary Documents.

Author Contributions

LS, YW and HW designed the research study. LS, YZ and YW performed the research. LS and YZ conducted experiments. LS and YW analyzed the data. All authors contributed to editorial changes in the manuscript. All authors read and approved the final manuscript. All authors have participated sufficiently in the work and agreed to be accountable for all aspects of the work.

Ethics Approval and Consent to Participate

Not applicable.

Acknowledgment

Not applicable.

Funding

This work was supported by the project of department of health of Hebei Province (20200196), excellent youth fund for basic scientific research projects of Hebei North University (JYT2021005), youth fund for basic scientific research projects of Hebei North University (JYT2022008) and the Project of Hebei North University (H2022405030), China.

Conflict of Interest

The authors declare no conflict of interest.

Supplementary Material

Supplementary material associated with this article can be found, in the online version, at https://doi.org/10.31083/j.jin2206136.

References

[1] Xue C, Gu X, Bao Z, Su Y, Lu J, Li L. The Mechanism Underlying the ncRNA Dysregulation Pattern in Hepatocellular Carcinoma and Its Tumor Microenvironment. Frontiers in Immunology. 2022; 13: 847728.

[2] Canseco-Rodriguez A, Masola V, Aliperti V, Meseguer-Beltran M, Donizetti A, Sanchez-Perez AM. Long Non-Coding RNAs, Extracellular Vesicles and Inflammation in Alzheimer's Disease. International Journal of Molecular Sciences. 2022; 23: 13171.

[3] Fontemaggi G. Non-coding RNA regulatory networks in post-transcriptional regulation of VEGFA in cancer. International Union of Biochemistry and Molecular Biology Life. 2023; 75: 30–39.

[4] Su L, Li R, Zhang Z, Liu J, Du J, Wei H. Identification of altered exosomal microRNAs and mRNAs in Alzheimer's disease. Ageing Research Reviews. 2022; 73: 101497.

[5] Zhang Q, Chen B, Yang P, Wu J, Pang X, Pang C. Bioinformatics-based study reveals that AP2M1 is regulated by the circRNA-miRNA-mRNA interaction network and affects Alzheimer's disease. Frontiers in Genetics. 2022; 13: 1049786.

[6] Dong LX, Zhang YY, Bao HL, Liu Y, Zhang GW, An FM. LncRNA NEAT1 promotes Alzheimer's disease by down regulating micro-27a-3p. American Journal of Translational Research. 2021; 13: 8885–8896.

[7] Canseco-Rodriguez A, Masola V, Aliperti V, Meseguer-Beltran M, Donizetti A, Sanchez-Perez AM. Long Non-Coding RNAs, Extracellular Vesicles and Inflammation in Alzheimer's Disease. International Journal of Molecular Sciences. 2022; 23: 13171.

[8] Klyucherev TO, Olszewski P, Shalimova AA, Chubarev VN, Tarasov VV, Attwood MM, *et al*. Advances in the development of new biomarkers for Alzheimer's disease. Translational Neurodegeneration. 2022; 11: 25.

[9] Koh HS, Lee S, Lee HJ, Min JW, Iwatsubo T, Teunissen CE, *et al*. Targeting MicroRNA-485-3p Blocks Alzheimer's Disease Progression. International Journal of Molecular Sciences. 2021; 22: 13136.

[10] Liang C, Zou T, Zhang M, Fan W, Zhang T, Jiang Y, *et al*. MicroRNA-146a switches microglial phenotypes to resist the pathological processes and cognitive degradation of Alzheimer's disease. Theranostics. 2021; 11: 4103–4121.

[11] Li Y, Wang H, Chen L, Wei K, Liu Y, Han Y, *et al*. Circ_0003611 regulates apoptosis and oxidative stress injury of Alzheimer's disease via miR-383-5p/KIF1B axis. Metabolic Brain Disease. 2022; 37: 2915–2924.

[12] Shen X, He Y, Ge C. Role of circRNA in pathogenesis of Alzheimer's disease. Journal of Central South University. Medical Sciences. 2022; 47: 960–966. (In English, Chinese)

[13] Song C, Zhang Y, Huang W, Shi J, Huang Q, Jiang M, *et al*. Circular RNA Cwc27 contributes to Alzheimer's disease pathogenesis by repressing Pur-α activity. Cell Death and Differentiation. 2022; 29: 393–406.

[14] Zeng T, Ni H, Yu Y, Zhang M, Wu M, Wang Q, *et al*. BACE1-AS prevents BACE1 mRNA degradation through the sequestration of BACE1-targeting miRNAs. Journal of Chemical Neuroanatomy. 2019; 98: 87–96.

[15] Twayana S, Legnini I, Cesana M, Cacchiarelli D, Morlando M, Bozzoni I. Biogenesis and function of non-coding RNAs in muscle differentiation and in Duchenne muscular dystrophy. Biochemical Society Transactions. 2013; 41: 844–849.

[16] Lai Y, He S, Ma L, Lin H, Ren B, Ma J, *et al*. HOTAIR functions as a competing endogenous RNA to regulate PTEN expression by inhibiting miR-19 in cardiac hypertrophy. Molecular and Cellular Biochemistry. 2017; 432: 179–187.

[17] Szklarczyk D, Gable AL, Nastou KC, Lyon D, Kirsch R, Pyysalo S, *et al*. The STRING database in 2021: customizable protein-protein networks, and functional characterization of user-uploaded gene/measurement sets. Nucleic Acids Research. 2021; 49: D605–D612.

[18] Shannon P, Markiel A, Ozier O, Baliga NS, Wang JT, Ramage D, *et al*. Cytoscape: a software environment for integrated models of biomolecular interaction networks. Genome Research. 2003; 13: 2498–2504.

[19] Chin CH, Chen SH, Wu HH, Ho CW, Ko MT, Lin CY. cytoHubba: identifying hub objects and sub-networks from complex interactome. BMC Systems Biology. 2014; 8: S11.

[20] Wang F, Xu CS, Chen WH, Duan SW, Xu SJ, Dai JJ, *et al*. Identification of Blood-Based Glycolysis Gene Associated with Alzheimer's Disease by Integrated Bioinformatics Analysis. Journal of Alzheimer's Disease. 2021; 83: 163–178.

[21] Agarwal V, Bell GW, Nam JW, Bartel DP. Predicting effective microRNA target sites in mammalian mRNAs. eLife. 2015; 4: e05005.

[22] Sticht C, De La Torre C, Parveen A, Gretz N. miRWalk: An online resource for prediction of microRNA binding sites. PLoS ONE 2018; 13: e0206239.

[23] Zhang Y, Qian L, Liu Y, Liu Y, Yu W, Zhao Y. CircRNA-ceRNA Network Revealing the Potential Regulatory Roles of CircRNA in Alzheimer's Disease Involved the cGMP-PKG Signal Pathway. Frontiers in Molecular Neuroscience. 2021; 14: 665788.

[24] Sun T, Zeng L, Cai Z, Liu Q, Li Z, Liu R. Comprehensive analysis of dysregulated circular RNAs and construction of a ceRNA

network involved in the pathology of Alzheimer's disease in a 5 × FAD mouse model. Frontiers in Aging Neuroscience. 2022; 14: 1020699.

[25] Ma N, Tie C, Yu B, Zhang W, Wan J. Identifying lncRNA-miRNA-mRNA networks to investigate Alzheimer's disease pathogenesis and therapy strategy. Aging. 2020; 12: 2897–2920.

[26] Ou GY, Lin WW, Zhao WJ. Construction of Long Noncoding RNA-Associated ceRNA Networks Reveals Potential Biomarkers in Alzheimer's Disease. Journal of Alzheimer's Disease. 2021; 82: 169–183.

[27] Bouakaz L, Bouakaz E, Murgola EJ, Ehrenberg M, Sanyal S. The role of ribosomal protein L11 in class I release factor-mediated translation termination and translational accuracy. The Journal of Biological Chemistry. 2006; 281: 4548–4556.

[28] Rao S, Peri S, Hoffmann J, Cai KQ, Harris B, Rhodes M, *et al*. RPL22L1 induction in colorectal cancer is associated with poor prognosis and 5-FU resistance. PLoS ONE. 2019; 14: e0222392.

[29] Oliveira MM, Klann E. eIF2-dependent translation initiation: Memory consolidation and disruption in Alzheimer's disease. Seminars in Cell and Developmental Biology. 2022; 125: 101–109.

[30] Wang X, Xia W, Li K, Zhang Y, Ge W, Ma C. Rapamycin regulates cholesterol biosynthesis and cytoplasmic ribosomal proteins in hippocampus and temporal lobe of APP/PS1 mouse. Journal of the Neurological Sciences. 2019; 399: 125–139.

[31] Suzuki M, Tezuka K, Handa T, Sato R, Takeuchi H, Takao M, *et al*. Upregulation of ribosome complexes at the blood-brain barrier in Alzheimer's disease patients. Journal of Cerebral Blood Flow and Metabolism. 2022; 42: 2134–2150.

[32] Meng F, Lu W, Yu F, Kang M, Guo X, Xu B. Ribosomal protein L11 is related to brain maturation during the adult phase in Apis cerana cerana (Hymenoptera, Apidae). Die Naturwissenschaften. 2012; 99: 343–352.

[33] Slomnicki LP, Hallgren J, Vashishta A, Smith SC, Ellis SR, Hetman M. Proapoptotic Requirement of Ribosomal Protein L11 in Ribosomal Stress-Challenged Cortical Neurons. Molecular Neurobiology. 2018; 55: 538–553.

[34] Hossain MB, Islam MK, Adhikary A, Rahaman A, Islam MZ. Bioinformatics Approach to Identify Significant Biomarkers, Drug Targets Shared Between Parkinson's Disease and Bipolar Disorder: A Pilot Study. Bioinformatics and Biology Insights. 2022; 16: 11779322221079232.

[35] Anderson SJ, Lauritsen JPH, Hartman MG, Foushee AMD, Lefebvre JM, Shinton SA, *et al*. Ablation of ribosomal protein L22 selectively impairs alphabeta T cell development by activation of a p53-dependent checkpoint. Immunity. 2007; 26: 759–772.

[36] Brunsing R, Omori SA, Weber F, Bicknell A, Friend L, Rickert R, *et al*. B- and T-cell development both involve activity of the unfolded protein response pathway. The Journal of Biological Chemistry. 2008; 283: 17954–17961.

[37] Novetsky AP, Zighelboim I, Thompson DM, Jr, Powell MA, Mutch DG, Goodfellow PJ. Frequent mutations in the RPL22 gene and its clinical and functional implications. Gynecologic Oncology. 2013; 128: 470–474.

[38] Hamed M, Gladbach Y, Möller S, Fischer S, Ernst M, Struckmann S, *et al*. A workflow for the integrative transcriptomic description of molecular pathology and the suggestion of normalizing compounds, exemplified by Parkinson's disease. Scientific Reports. 2018; 8: 7937.

[39] Duarte RRR, Bachtel ND, Côtel MC, Lee SH, Selvackadunco S, Watson IA, *et al*. The Psychiatric Risk Gene NT5C2 Regulates Adenosine Monophosphate-Activated Protein Kinase Signaling and Protein Translation in Human Neural Progenitor Cells. Biological Psychiatry. 2019; 86: 120–130.

[40] Anirudhan A, Angulo-Bejarano PI, Paramasivam P, Manokaran K, Kamath SM, Murugesan R, *et al*. RPL6: A Key Molecule Regulating Zinc- and Magnesium-Bound Metalloproteins of Parkinson's Disease. Frontiers in Neuroscience. 2021; 15: 631892.

[41] Hou G, Lu Z, Jiang J, Yang X. Ribosomal protein L32 enhances hepatocellular carcinoma progression. Cancer Medicine. 2023; 12: 10791–10803.

[42] Barkić M, Crnomarković S, Grabusić K, Bogetić I, Panić L, Tamarut S, *et al*. The p53 tumor suppressor causes congenital malformations in Rpl24-deficient mice and promotes their survival. Molecular and Cellular Biology. 2009; 29: 2489–2504.

[43] Zhou X, Liu Z, He T, Zhang C, Jiang M, Jin Y, *et al*. DDX10 promotes the proliferation and metastasis of colorectal cancer cells via splicing RPL35. Cancer Cell International. 2022; 22: 58.

[44] Wu W, Yu N, Li F, Gao P, Lin S, Zhu Y. RPL35 promotes neuroblastoma progression via the enhanced aerobic glycolysis. American Journal of Cancer Research. 2021; 11: 5701–5714.

[45] Sharen G, Li X, Sun J, Zhang L, Xi W, Zhao X, *et al*. Silencing eL31 suppresses the progression of colorectal cancer via targeting DEPDC1. Journal of Translational Medicine. 2022; 20: 493.

[46] Farrar JE, Nater M, Caywood E, McDevitt MA, Kowalski J, Takemoto CM, *et al*. Abnormalities of the large ribosomal subunit protein, Rpl35a, in Diamond-Blackfan anemia. Blood. 2008; 112: 1582–1592.

[47] Mirzaei M, Pushpitha K, Deng L, Chitranshi N, Gupta V, Rajput R, *et al*. Upregulation of Proteolytic Pathways and Altered Protein Biosynthesis Underlie Retinal Pathology in a Mouse Model of Alzheimer's Disease. Molecular Neurobiology. 2019; 56: 6017–6034.

[48] Lu L, Dai WZ, Zhu XC, Ma T. Analysis of Serum miRNAs in Alzheimer's Disease. American Journal of Alzheimer's Disease and other Dementias. 2021; 36: 15333175211021712.

[49] Liu Q, Zhu L, Liu X, Zheng J, Liu Y, Ruan X, *et al*. TRA2A-induced upregulation of LINC00662 regulates blood-brain barrier permeability by affecting ELK4 mRNA stability in Alzheimer's microenvironment. RNA Biology. 2020; 17: 1293–1308.

[50] AmeliMojarad M, AmeliMojarad M, Pourmahdian A. Circular RNA circ_0051620 sponges miR-338-3p and regulates ADAM17 to promote the gastric cancer progression. Pathology, Research and Practice. 2022; 233: 153887.